

# Strategies for quantitative NO-concentration and temperature measurements by NO LIF in high-pressure flames

W. G. Bessler\*, T. Lee, C. Schulz\*, J.B. Jeffries\*\*, and R.K. Hanson  
High Temperature Gasdynamics Laboratory, Mechanical Engineering Department  
Stanford University, Stanford, CA 94305-3032

## Abstract

At pressures above 10 atmospheres, attenuation of the excitation laser and fluorescence signal in the hot combustion gases and interference from molecular oxygen LIF causes significant problems for NO LIF. We present a detailed comparison of various strategies for NO-LIF exploring the choices of excitation and detection transitions in the A-X (0,0), (0,1), and (0,2) bands. Using spectroscopic measurements in laminar premixed methane/air flames at pressures between 1 and 60 bar, we discuss the advantages and problems of the detection strategies in terms of spectral purity, pressure and temperature influence, and susceptibility to laser and signal light attenuation. The selected strategies are then used for quantitative NO-concentration- and temperature-imaging in high pressure flames.

## Introduction

Air-breathing engines provide modern man with unprecedented mobility at the societal expense of air pollution from the combustion effluent and consumption of hydrocarbon fuels. The optimization of pollutant formation often comes at a cost to fuel economy, and simultaneous minimization of pollutant emissions and maximization of fuel consumption is an important research topic for all engine designs. Nitric oxide (NO) is one of the most important combustion generated air pollutants, and quantitative tools for spatially resolved *in situ* NO measurements are quite desirable for this research. Laser-induced fluorescence is a widely used tool for such measurements, and NO LIF is quite straight-forward at atmospheric pressure [1-3]. Unfortunately as the pressure increases, NO LIF is plagued with absorption of the excitation laser and LIF fluorescence signal and interference LIF from other species in combustion effluent. There is a long and rich literature on high-pressure NO LIF, which is reviewed in ref. [4] and the references therein.

Recently we conducted an extensive research effort to understand the optimization of the LIF excitation/detection strategy for quantitative LIF of NO in high-pressure hydrocarbon combustion environments. That work included careful consideration of NO excitation strategies[4], high-pressure flame investigation of NO excitation in the A-X system in the (0,0)[5], (0,1)[6], and (0,2)[7,8] bands, measurements of absorption by combustion effluent [9-11], identification of CO<sub>2</sub> LIF interference [12], comprehensive spectroscopic model development [13], and the demonstration of quantitative NO LIF imaging [14,15]. In this paper we review the issues for quantitative determination of gas temperature and concentration using NO-LIF in high-pressure combustion.

## Background

### A. Signal strength and signal interference

LIF measurements of NO are faced with difficulties in selectivity. This is true especially in high-pressure combustion environments, where laser-induced emission not only from NO but also from other species present in the flame becomes important if not dominant. Using an appropriate excitation wavelength and detection bandpass is crucial to maximize signal strength and minimize potential interference. There are three primary sources of signal interference, and their influence depends on the specific combustion situation.

1. O<sub>2</sub>-LIF interference. Hot O<sub>2</sub> is the main contributor to LIF interference in lean and non-premixed flames. The  $B^3\Sigma^- - X^3\Sigma^+$  Schumann-Runge bands of O<sub>2</sub> overlap with the  $A^2\Sigma^+ - X^2\Pi$  NO gamma bands over a wide range of excitation wavelengths [1] resulting in overlapping absorption features and fluorescence signals. Because the fluorescence lifetime of the relevant excited states of O<sub>2</sub> is limited by predissociation, the pressure influence on line broadening and fluorescence quantum yield is much smaller than for NO. This leads to an increase of the relative contribution of O<sub>2</sub>-LIF background with increasing pressure [5]. To avoid this interference problem with broad-band LIF detection, a careful choice of excitation transition is necessary. Furthermore, different strategies have been suggested to correct for remaining interference.
2. CO<sub>2</sub> broadband LIF emission was recently identified in lean, stoichiometric and rich high-pressure methane/air and methane/oxygen/argon flames[12]. The LIF signal consists of a broad (200-450 nm) continuum with a faint superimposed band structure, and its fluorescence yield is constant for pressures up to at least 40 bar. The

\* Permanent address: Physikalisch-Chemisches Institut, Universität Heidelberg, INF 253, 69120 Heidelberg

\*\* Corresponding author: Jay B. Jeffries, Jay.Jeffries@Stanford.edu

Proceedings of the Third Joint Meeting of the U.S. Sections of The Combustion Institute

relative influence of the CO<sub>2</sub> LIF increases with pressure just like O<sub>2</sub> because the NO fluorescence yield is proportional to  $1/p$ . Although the signal is comparatively weak, it can become an important contribution to the overall signal when detection over wide spectral ranges is used.

3. PAH-LIF interference in rich flames. In rich and non-premixed flames additional broad-band fluorescence interference has been observed which is usually attributed to polycyclic aromatic hydrocarbons (PAHs) and partially burned hydrocarbons (aldehydes, ketones) [16]. In sooting flames at high laser energies, interference by LIF of laser-generated C<sub>2</sub> has also been reported [17]. Laser-induced incandescence (LII) is observed in sooting flames [18], however at considerably longer wavelengths ( $> 350$  nm) than normally used for NO detection ( $< 300$  nm). The work reported here concentrates on premixed flames with the equivalence ratio  $\phi < 1.2$  where the PAH interference is relatively minor. Work on CO<sub>2</sub> LIF [12] shows the onset of strong PAH interference near  $\phi = 1.6$ .

Appropriate choice of NO-LIF signal detection wavelength is most important for the discrimination against interfering signals. With A-X(0,0) excitation, detection is possible only at longer wavelengths (red-shifted) relative to the excitation wavelengths. Excitation within the A-X(0,1) and (0,2) bands offers the possibility for blue-shifted detection, leading to more effective suppression of CO<sub>2</sub>- and PAH-LIF signals which occur almost exclusively red-shifted relative to the excitation wavelength

#### *B. Transmission properties for A-X excitation light*

The relatively short laser wavelengths used to electronically excite NO are strongly absorbed in high-temperature, high-pressure combustion environments. Recently was it recognized that the main absorbing species are hot CO<sub>2</sub> and H<sub>2</sub>O present in the combustion gases. Absorption cross sections increase with temperature and decrease with wavelength [10]. The effect increases with pressure due to the increasing number density of absorbers, leading to strong attenuation of both laser and signal light even in small flame geometries [11,14]. These observations made clear that excitation at longer wavelengths are desirable and that excitation in the D-X band at 193 nm can not be recommended for flame diagnostics at elevated pressures. Therefore we focus here on a comparison of A-X excitation bands (NO A-X(0,0), (0,1) and (0,2) at around 226, 237 and 248 nm respectively). Since excitation within these bands all populate the same excited vibrational level ( $v' = 0$ ), quenching and excited state energy transfer processes and therefore signal interpretation are similar for these approaches. However, a careful consideration of signal interference and temperature dependence is necessary to assess the feasibility of these different approaches.

#### *C. Interpretation and quantification of NO LIF signals*

The conversion of measured NO-LIF intensities to relative NO concentrations requires correction for the influence of temperature, pressure, and the concentrations of all other species; furthermore, calibration of the relative concentrations is required for quantitative NO concentration measurements to account for the collection optics, detector quantum efficiency, laser energy density, etc.

The main temperature dependence of the NO-LIF signal strength arises from the Boltzmann distribution of ground state population. Collisional (pressure) broadening and line-shifting have been measured for the NO A-X band for collisions with the main combustion species and are included in the spectral simulation [13]. Variations in pressure, temperature, and (less importantly) gas phase composition influence the spectral overlap of the laser line profile with the NO absorption features. As a result, excitation efficiency and therefore LIF signal decreases with increasing pressure. Collisional fluorescence quenching of the NO A state has been investigated in detail [19], and models have been established and validated to describe the effects of temperature and colliding species on quenching cross sections [20]. The quenching rate scales with pressure. The fluorescence quantum yield of the NO A state decreases strongly with increasing pressure, and further varies with temperature and gas composition.

Pressure can be measured accurately in most situations and with high temporal resolution using piezoelectric sensors, and the correction of the LIF signals for pressure is therefore feasible. The measurement of temperature, on the other hand, requires a large experimental effort, and it is usually not feasible to obtain temperature information simultaneously with NO-LIF data in practical, often turbulent, applications. Modeled temperatures can be used for correcting NO-LIF intensities, however, the accuracy is severely limited in unsteady flames. Thus, quantitative NO concentration measurements without the exact knowledge of local temperature often require choosing a transition which minimizes the total temperature sensitivity of the LIF signal. This does not necessarily mean choosing a level with a population with minimum temperature sensitivity. In some cases a systematic variation of the ground state population with temperature might be desired to compensate for other temperature-dependent effects.

Even less available than temperature is the concentration of colliding species. While chemical simulations are feasible in laminar flames, NO LIF in turbulent combustion situations normally cannot be corrected for composition fluctuations. The introduced error is, however, relatively small for premixed combustion since NO is present only in the post-flame-front gases where the majority species concentrations are known relatively precisely.

## Experiment

The experimental set-up is identical to the ones previously used [4-6]. Laminar, premixed methane/air flat-flames for fuel/air equivalence ratios of  $\phi = 0.83, 0.93, 1.03$  and  $1.13$  and pressures from 1 to 60 bar were stabilized on a porous, sintered stainless steel plate of 8 mm diameter; in a 60 mm diameter stainless steel housing with pressure stabilization  $\pm 0.1$  bar. To mimic engine-like conditions, 300 ppm NO was seeded to the feedstock gases. A Nd:YAG-pumped frequency-doubled dye laser produced laser light (ca. 1 mJ,  $0.4 \text{ cm}^{-1}$  full width at half maximum, fwhm). The laser beam passed parallel to the burner 2 mm above the matrix. Fluorescence signals were line-imaged onto the horizontal entrance slit of a 250 mm imaging spectrometer, and the dispersed fluorescence signals were detected with an intensified CCD camera. Each laser pulse yielded a complete fluorescence spectrum maintaining one-dimensional spatial resolution along the laser light path. In these images the central area of the flame where temperature and concentrations are homogeneous was then chosen and integrated over the spatial axis, yielding a point on the fluorescence spectrum.

The laser was tuned to record excitation spectra in a  $\pm 0.0125 \text{ nm}$  range around specific NO transitions within the A-X bands (for the (0,0) band the blend of  $P_1(23.5)$ ,  $Q_1+P_{21}(14.5)$ ,  $Q_2+R_{12}(20.5)$  near 226.03 nm, for the (0,1) the  $P_1(25.5)$ ,  $R_1+Q_{21}(11.5)$ ,  $Q_1+P_{21}(17.5)$  near 235.87 nm, and for the (0,2) the  $O_{12}(7.5-10.5)$  bandhead near 247.94 nm). This choice is based on previous results and simulation calculations as described in Refs. [5] and [6]. The signal was averaged over 20-50 laser pulses for each excitation wavelength and stored for further evaluation before scanning the laser to the next wavelength.

The emission spectra at excitation wavelengths corresponding to maximum NO-LIF intensities were evaluated to separate and quantify the overlapping LIF signals of NO,  $O_2$ , and  $CO_2$ . Raman signals were not observed in the hot flame gases (the laser was polarized horizontally for maximum suppression of the Raman signal). The experimental data were corrected for the wavelength-dependent detection efficiency and signal absorption from hot exhaust gases [10]. A non-linear least-squares fitting procedure was used to separate the various overlapping LIF spectra and the contribution of elastically scattered light (Rayleigh), and to account for the (Voigt-type) spectrograph slit function. The intensities of simulated NO- and  $O_2$ -LIF emission spectra [13], experimental  $CO_2$ -LIF emission spectra [12], and a Rayleigh signal were simultaneously fitted to the experimental data. The  $O_2$ -LIF emission spectra are complex due to overlapping absorption lines leading to simultaneous excitation into multiple vibrational states. Furthermore, vibrational energy transfer in the upper electronic (B) state was evident from the  $O_2$ -LIF emission structure. Therefore, emission signals from multiple upper vibrational  $O_2$  B-states were fitted

independently. Fig. 1 shows emission spectra and fitting results for the excitation strategies compared in this paper for lean 60 bar flames.

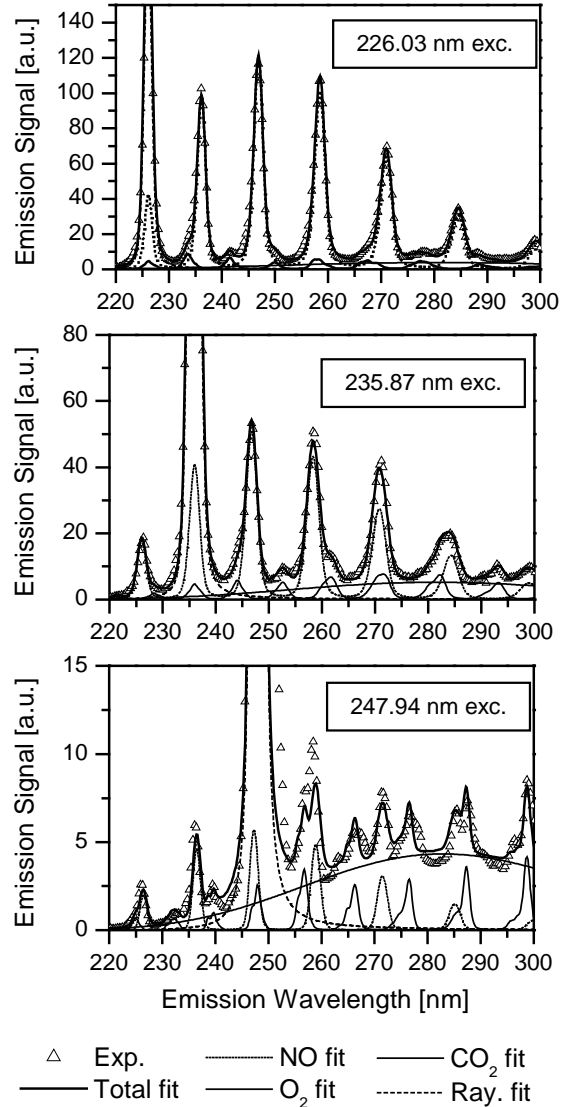


Fig. 1: Examples of the nonlinear least-square fit of simulated NO,  $O_2$ ,  $CO_2$ , and Rayleigh emission spectra (represented as Voigt line shapes) for the investigated excitation strategies at  $p = 60 \text{ bar}$ ,  $\phi = 0.83$ . The intensity is on the same scale in all panels.

## Results

We compare one excitation strategy within each of the A-X(0,0), (0,1) and (0,2) bands that was shown previously to yield best performance in terms of signal strength and interference suppression [5,6]. For each excitation scheme, different detection strategies relevant for band-pass-filtered imaging in practical application are com-

pared. With (0,0) excitation only red-shifted detection is possible, but for (0,1) and (0,2) excitation we compare both red- and blue-shifted detection. In particular, we simulate 20-nm-bandpass detection of two NO vibrational emission bands (except for blue-shifted detection after (0,1) excitation where only one band can be detected).

Usually, bandpass detection of the LIF signal is performed, acquiring the emission of one or more vibrational emission bands. The signal strength can easily be increased by detection of multiple bands (usually at the cost of increased interference). In many high-pressure burner applications, on the other hand, point measurements using narrow-band monochromator detection were performed. This strategy yields better signal/interference ratios at the cost of signal strength. When complete emission spectra are recorded (e.g. by using an imaging spectrograph like in this work), the selectivity can be further enhanced by fitting the different contributions of interfering species to the spectra prior to evaluating the NO-LIF intensity. A comparison of these strategies is not attempted here.

#### A. Signal strength in non-absorbing environments

NO LIF signal strength is maximized by choosing a ground state with a large population at flame temperatures and transition with a large oscillator strength. At typical combustion temperatures in the range 1500 – 2500 K, the largest vibrational population is present in the  $X \nu'' = 0$  level. The  $\nu'' = 1$  and 2 levels have respective energies of 1846 and 3724  $\text{cm}^{-1}$  above the ground state, corresponding to maximum populations at  $\sim 2700$  and  $\sim 5400$  K. Largest lower state populations are therefore found in the A-X(0,0) band in most combustion applications. Since NO LIF involves excitation with narrow-bandwidth lasers, the relevant population is that for the lower level of a particular rovibrational transition. Furthermore, absorption features consisting of multiple, overlapped transitions (e.g. band heads) can easily be found in the NO spectra and these blends yield stronger signals than single transitions for pressures up to ca. 40 bar (before pressure broadening becomes dominant).

In high-pressure systems, where line broadening and -shifting severely influence the excitation efficiency, an optimized strategy for NO LIF should involve excitation at a wavelength yielding maximum signal strength for each individual pressure. Since pressure shift is in the range of 0.2  $\text{cm}^{-1}/\text{bar}$  [21-24], this means tuning the laser by several wavenumbers in typical pressure ranges of 10 – 50 bar when exciting at the peak of a single, isolated transition. In practical applications, however, pressure often varies rapidly (e.g. in internal combustion engines). Here, a fixed excitation wavelength must be chosen. The resulting signal loss is most pronounced for pressures between 1 and 5 bar due to the simultaneous action of pressure broadening and -shift. This effect may partly be reduced by choosing broad, multi-line absorption features [5].

Fig. 2 shows measured and simulated signal strengths for the different A-X strategies for excitation in a 10 bar flame, normalized to the signal strength of the (0,0) approach. The simulations have been performed for a typical flame temperature of 1900 K [14]. A-X(0,0) strategies clearly show the strongest signals, A-X(0,1) excitation yields signal intensities about an order of magnitude lower. Signal is decreased by another order of magnitude with A-X(0,2) excitation. The difference between red- and blue-shifted detection reflects the different Franck-Condon factors.

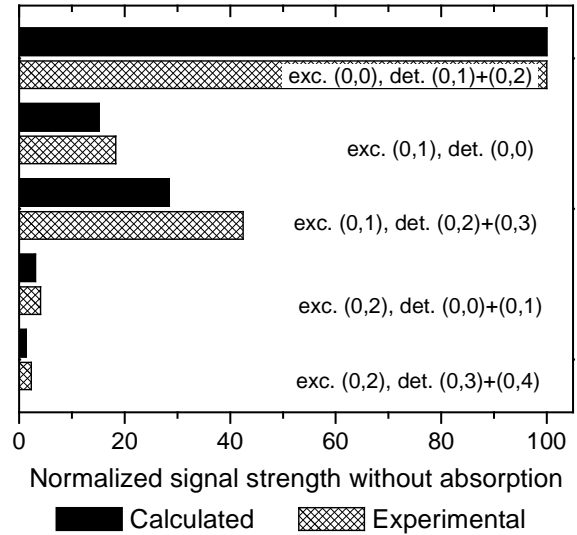


Fig. 2: Calculated and experimental signal strengths for the 10 bar flame. Exc.: excited, det.: detected vibrational band within the NO A-X system.

Considering signal strength alone, (0,0) excitation is clearly the strategy of choice. However, in the hot post-flame combustion gas where absorption coefficients are strongly wavelength-dependent, the other strategies should not be discarded simply on the basis of signal strength. Furthermore, the high laser power of the tunable excimer laser usually used for (0,2) excitation may partially compensate for the low signal strength for imaging measurements where the output of dye lasers limits the excitation energy for the laser sheet.

#### B. Influence of attenuation by hot $\text{CO}_2$ and $\text{H}_2\text{O}$

Hot combustion products like  $\text{CO}_2$  and  $\text{H}_2\text{O}$  have long been ignored as potential absorbers in laser-based combustion diagnostics work. However, at wavelengths shorter than 250 nm for  $\text{CO}_2$  and shorter than 230 nm for  $\text{H}_2\text{O}$  their influence becomes relevant at flame temperatures and increases towards shorter wavelengths [9-11]. This causes attenuation of the laser as well as the fluorescence light. The transmission depends not only on the

wavelength, but also on the path length and therefore on flame geometry and experimental configuration. This produces nearly opposite effects: With (0,0) excitation and red-shifted detection, strong laser attenuation with less signal attenuation occurs; with (0,2) excitation and blue-shifted detection, laser attenuation is less but signal attenuation is stronger. For a quantitative comparison, laser and signal transmission are calculated for flame center measurements in two typical high-pressure flame configurations:

- **Case 1:** High-pressure burner, 40 bar, 1900 K, 8 mm diameter (e.g., Ref. [14])
- **Case 2:** DI Diesel engine, 50 bar, 2400 K, 80 mm diameter, laser travels through cylinder window, detection through piston window (e.g., Ref. [25])

The calculations are performed using the expressions given in ref. [10] for  $\phi = 0.9$  equilibrium exhaust gas concentrations of  $\text{CO}_2$  and  $\text{H}_2\text{O}$ . The different influence on laser and signal wavelengths can clearly be followed: In case 1, the high-pressure flame, total transmission (laser and signal) varies between 75 and 92% for the investigated strategies, and the difference between (0,0) excitation / (0,1),(0,2) detection and (0,2) excitation / (0,0),(0,1) detection is small (75% vs. 82% total transmission). In case 2, the Diesel engine, absorption is much stronger because of the higher temperatures and longer paths involved. In this geometry with long laser path and short signal path (detection through piston window), (0,0) excitation has a strong disadvantage. In this case there is a large difference when comparing (0,0) excitation / (0,1),(0,2) detection and (0,2) excitation / (0,0),(0,1) detection, the latter strategy yielding a total transmission of 26 times that of the former.

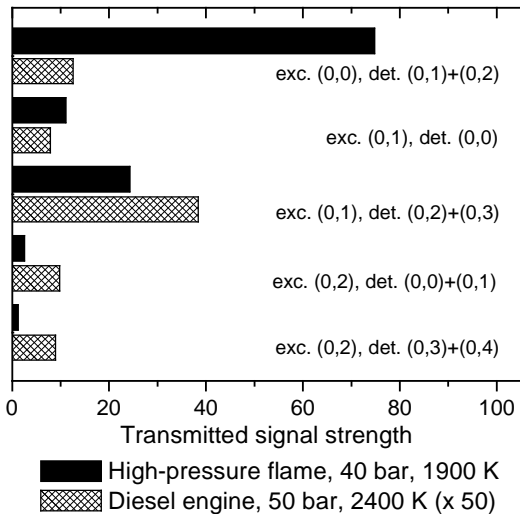


Fig. 3: Calculated signal strengths after laser and signal absorption by hot  $\text{CO}_2$  and  $\text{H}_2\text{O}$ , normalized to the (0,0) strategy signal without absorption. Exc.: excited, det.: detected vibrational band within the NO A-X system.

Fig. 3 gives relative signal strengths, normalized to the signal strength of the (0,0) strategy without absorption. In the high-pressure flame the strong difference in signal strength in non-absorbing environments persists; however, in the Diesel engine signal strengths are all within the same order of magnitude. Longer-wavelength excitation should be preferred here because the overall transmission is much larger and signals are therefore less influenced by fluctuations of pressure or temperature.

It is important to emphasize that the transmission properties strongly depend on the specific combustion situation (pressure, temperature) and experimental geometry (laser and signal paths). In internal combustion engines, for example, signal transmission may increase, decrease or stay constant with piston position (crank angle degree) due to the simultaneous variation of pressure, temperature, and path length, depending on the position of the laser beam above the piston window. The advantage of long-wavelength excitation is most pronounced at very high pressure (above ca. 40 bar) and long laser path lengths.

### Conclusions

We compared five practical schemes for NO A-X LIF exciting transitions in the (0,0), (0,1) and (0,2) bands and detection red- and blue-shifted relative to the excitation wavelength. No single “best strategy” can be recommended for all combustion situations. The choice is a trade-off between selectivity and signal intensity on one hand and the optical accessibility in terms of laser and signal absorption on the other hand. The properties of the strategies compared in this work can be summarized as follows.

- The A-X (0,0) approach (excitation at 226.03 nm, only red-shifted detection possible) clearly offers the best performance in terms of signal strength and selectivity. It is the strategy of choice for combustion diagnostics at all pressures as long as laser attenuation is acceptably low. It is therefore especially suitable for high-pressure combustion with small flame diameters. The temperature sensitivity allows measurement of NO number densities even without detailed knowledge of local temperatures. However at high pressures and temperatures ( $> 40$  bar,  $> 2200$  K), especially in internal combustion engines, laser attenuation may reach levels that make quantitative or even qualitative measurements impossible using the (0,0) excitation strategy. The red-shifted detection of potential PAH interference may further complicate this approach.
- The A-X (0,1) approach (excitation at 235.87 nm) with red-shifted detection is very attractive, although it has only scarcely been applied. It offers relatively strong signals (about 1/3 of the (0,0) approach) and at the same time reduces attenua-

tion of both laser and signal light, especially if the experiment requires long signal paths. Signal purity is still good at intermediate NO concentrations (around 300 ppm). The temperature sensitivity allows measurement of NO mole fractions even without detailed knowledge of local temperatures. However, this red-shifted detection scheme may allow unwanted PAH interference.

- The A-X (0,2) approach (excitation at 247.94 nm) with blue-shifted detection has been widely employed in high-pressure high-temperature combustion situations. Although the signal strength is low, it strongly reduces attenuation problems in typical in-cylinder experimental geometries with long laser path and short signal path. Interference levels are acceptable for high NO concentrations ( $\geq 1000$  ppm). In addition, previous literature suggests that this approach is most effective to minimizing PAH interference.

### Acknowledgement

Work at Stanford is supported by the US Air Force Office of Scientific Research, Aerospace Sciences Directorate, with Julian Tishkoff as the technical monitor. The Division of International Programs at the US National Science Foundation supports the Stanford collaboration via a cooperative research grant. The University of Heidelberg work and the travel of WB and CS are sponsored by the Deutsche Forschungsgemeinschaft (DFG) and the Deutsche Akademische Auslandsdienst (DAAD).

### References

1. Eckbreth, A. C., *Laser diagnostics for combustion temperature and species*, 2 ed (Gordon and Breach, Amsterdam, The Netherlands, 1996).
2. Kohse-Höinghaus, K., *Progress In Energy And Combustion Science* 20:203 (1994).
3. Kohse-Höinghaus, K. and Jeffries, J. B., *Applied Combustion Diagnostics* (Taylor and Francis, New York, 2002).
4. Bessler, W. G., Schulz, C., Lee, T., Jeffries, J. B., and Hanson, R. K., *Appl. Opt.* submitted (2003).
5. Bessler, W. G., Schulz, C., Lee, T., Jeffries, J. B., and Hanson, R. K., *Appl. Opt.* 41:3547 (2002).
6. Bessler, W. G., Schulz, C., Lee, T., Jeffries, J. B., and Hanson, R. K., *Applied Optics* in press (2003).
7. Schulz, C., Sick, V., Heinze, J., and Stricker, W., *Appl. Opt.* 36:3227 (1997).
8. Schulz, C., Sick, V., Meier, U., Heinze, J., and Stricker, W., *Appl. Opt.* 38:434 (1999).
9. Hildenbrand, F. and Schulz, C., *Appl. Phys. B* 73:165 (2001).
10. Schulz, C., Koch, J. D., Davidson, D. F., Jeffries, J. B., and Hanson, R. K., *Chemical Physics Letters* 355:82 (2002).
11. Schulz, C., Jeffries, J. B., Davidson, D. F., Koch, J. D., Wolfrum, J., and Hanson, R. K., *Proc. Comb. Inst.* 29:in press (2002).
12. Bessler, W. G., Lee, T., Schulz, C., Jeffries, J. B., and Hanson, R. K. in *Proceedings of the Joint meeting of the US sections of the combustion institute* (2003), in preparation.
13. Bessler, W., G., Schulz, C., Sick, V., and Daily, J. W. in *Proceedings of the Proceedings of the 3rd Joint Meeting of the US Sections of the Combustion Institute* (2003).
14. Bessler, W. G., Schulz, C., Lee, T., Shin, D. I., Hofmann, M., Jeffries, J. B., Wolfrum, J., and Hanson, R. K., *Appl. Phys. B* 75:97 (2002).
15. Bessler, W. G., Schulz, C., Lee, T., Shin, D. I., Hofmann, M., Jeffries, J. B., Wolfrum, J., and Hanson, R. K. in *Proceedings of the 1st International conference on optical and laser diagnostics (ICOLAD)* (London, December 16-20, 2002).
16. Cialolo, A., Barbella, R., Tregrossi, A., and Bonfanti, L., *Proc. Comb. Inst.* 27:1481 (1998).
17. Bengtsson, P.-E. and Aldén, M., *Appl. Phys. B* 60:51 (1995).
18. Hofmann, M., Bessler, W. G., Schulz, C., and Jander, H., *Appl. Opt.* in press (2003).
19. Tamura, M., Berg, P. A., Harrington, J. E., Luque, J., Jeffries, J. B., Smith, G. P., and Crosley, D. R., *Combustion and Flame* 114:502 (1998).
20. Paul, P. H., Gray, J. A., Durant Jr., J. L., and Thoman Jr., J. W., *Appl. Phys. B* 57:249 (1993).
21. DiRosa, M. D. and Hanson, R. K., *J. Quant. Spectrosc. Radiat. Transfer* 52:515 (1994).
22. Chang, A. Y., DiRosa, M. D., and Hanson, R. K., *J. Quant. Spectrosc. Radiat. Transfer* 47:375 (1992).
23. DiRosa, M. D. and Hanson, R. K., *J. Mol. Spectrosc.* 164:97 (1994).
24. Vyrodov, A. O., Heinze, J., and Meier, U. E., *J. Quant. Spectrosc. Radiat. Transfer* 53:277 (1995).
25. Hildenbrand, F., Schulz, C., Wolfrum, J., Keller, F., and Wagner, E., *Proc. Combust. Inst.* 28:1137 (2000).